Sea-salt and dust aerosols in the ECMWF IFS model

J.-J. Morcrette,[1] A. Beljaars,[1] A. Benedetti,[1] L. Jones,[1] and O. Boucher[2]

Received 17 September 2008; revised 30 October 2008; accepted 18 November 2008; published 31 December 2008.

[1] The ECMWF IFS model has recently been modified to include prognostic aerosols in its analysis and forecast modules. For the sea salt and dust components, comparisons of three versions of the model are presented: (i) a forecast only model started from conventional analysis with free-running aerosols, (ii) a full analysis including aerosols, and (iii) as in (i) but with sea salt and dust sources revised to account for the 10-m wind including gustiness and calibrated on the aerosol analysis results. It is shown that this new formulation of the sources of the main natural aerosols gives an improved agreement with AERONET surface observations where sea salt and dust aerosols are dominant. It also shows how the information brought by the aerosol analysis can be used to improve the representation of aerosols in numerical weather prediction and climate-type general circulation models. **Citation:** Morcrette, J.-J., A. Beljaars, A. Benedetti, L. Jones, and O. Boucher (2008), Sea-salt and dust aerosols in the ECMWF IFS model, *Geophys. Res. Lett.*, *35*, L24813, doi:10.1029/2008GL036041.

1. Introduction

[2] A prognostic representation of aerosols was recently developed as an integral part of the ECMWF (European Centre for Medium-range Weather Forecasts) Integrated Forecast System (IFS) in both its analysis and forecast modules [*Morcrette et al.*, 2008; *Benedetti et al.*, 2008] accounting for sea salt (SS), dust (DU), organic and black carbon, and sulphate aerosols. In the original formulation of the ECMWF model as in that of most general circulation or transport models carrying prognostic aerosols, sources of SS and DU are linked to the wind at 10-meters (10W). Recently, the importance of accounting for gustiness in the surface wind used for diagnosing the surface flux of particles was stressed by *Engelstaedter and Washington* [2007] who showed a 70 percent stronger correlation of dust emission with gustiness than with 10-meter wind. Similar concern also exists for sea salt aerosols [*Marenco et al.*, 2007]. This study addresses the question whether a parameterization of sea salt and dust aerosol sources based on 10-m wind including gustiness (10WIG) and calibrated on an analysis of satellite-derived aerosol optical depth is beneficial to the representation of aerosol processes in a global atmospheric model. We present results from three series of forecasts, two for which aerosols are free to evolve based on their sources and sinks (hereafter referred to as free-running (*FR*) forecasts), and one where the aerosols are constrained every 12 hours by an analysis of MODIS-derived aerosol optical depth (hereafter referred to *AN*). The original free-running forecast (*FR*0) uses 10*W* as predictor for the emissions and an initial distribution of the dust emission potential (DEP), the second free-running forecast (*FRA*) uses 10WIG as predictor for the emissions and a distribution of DEP adjusted to give DU aerosol optical depths close to the ones resulting from the analysis. Conclusions on the usefulness of such aerosol analysis to improve the representation of aerosols in general circulation models are then drawn.

2. Model

[3] In this study, the ECMWF IFS model is used with a resolution of T_L159 $L60$ (i.e., a horizontal grid of [1.125 deg]^2 and 60 vertical levels from surface to 0.1 hPa). The model can be run in either free-running (*FR*) aerosols mode or analysis (*AN*) mode.

[4] In both configurations, sources of sea-salt and dust are interactive with surface and near-surface variables of the model. Other aerosol sources are taken from monthly-mean climatologies (Emission Database for Global Atmospheric Research, Speciated Particulate Emission Wizard) or eight-day mean inventories (Global Fire Emission Database). All aerosols undergo advection, sedimentation, and dry and wet deposition (this last one by large-scale and convective precipitation). For organic matter and black carbon, two components, hygrophobic and hygrophilic, are considered. SO_2 and SO_4 are considered with no explicit chemistry included.

[5] In *FR* mode (without previous aerosol analysis), the model is run from 1 December 2002 to 31 January 2005, in a series of 12-hour forecasts starting every 12 hours and taking surface pressure, temperature, humidity and wind information from the ECMWF operational analyses. The aerosols are started from null concentrations on 1 December 2002 at 00UTC, get produced from surface emission fluxes, and are free-running after that (i.e., the aerosols at the end of a given 12-hour forecast are passed as initial conditions at the start of the next 12-hour forecast).

[6] In aerosol AN mode, the analysis is also performed on the total aerosol mixing ratio, calculated as the sum of all aerosol species [*Benedetti et al.*, 2008]. The background fractional contributions (provided by the same forward model as discussed above, but from successive analyses every 12 hours) are then used to re-distribute the analysis increments of total mixing ratio into the single species. This is achieved through an aerosol mass adjustment using observations of total optical depth derived from the Moderate Resolution Imaging Spectroradiometer (MODIS) instrument on-board of NASA Terra and Aqua satellites. The aerosol observations are ingested through the operational pathway and ingested in the 4D-Var system where they are processed with an ad hoc observation operator specifically

[1]ECMWF, Reading, UK.
[2]Met Office, Hadley Centre, Exeter, UK.

0094-8276/08/2008GL036041$05.00

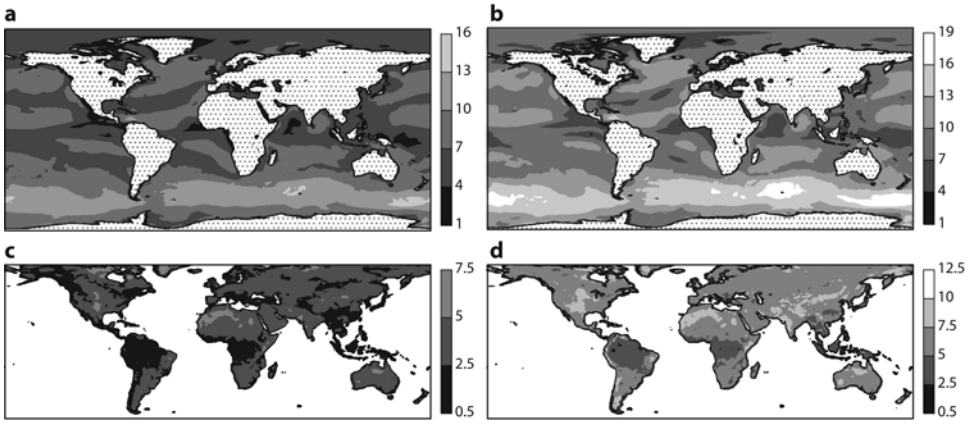

Figure 1. The wind at 10 meters for May 2003 (in m s^{-1}). (a) The 10-m wind over the ocean. (b) The 10-m wind including the gusts. (c) The 10-m wind over land. (d) The 10-m wind including the gusts over land. Note the different scales for ocean and land.

designed for aerosol optical depth. This operator uses precomputed values of optical properties, specific to the different aerosol species at the wavelengths of interest (subsequent results are only presented for 550 nm), in combination with the first-guess values of the aerosol mixing ratios from the model to calculate a profile of extinction. This extinction profile is then vertically integrated to obtain the total aerosol optical depth.

[7] Whatever the mode (*FR* or *AN*), sea salt and desert dust are each represented by three bins, whose limits (0.03 – 0.5 – 5 – 20 μm for sea salt and 0.03 – 0.55 – 0.9 – 20 μm for dust) are chosen as to have roughly 10, 20 and 70 percent of the mass of each aerosol type in the various bins. The surface flux of sea salt aerosols is parameterized from the 10-m wind at the free ocean surface following *Monahan et al.* [1982]. For the production of desert dust, the source follows an approach modified from *Ginoux et al.* [2001] and depends on the 10-m wind, soil moisture, the UV-visible component of the surface albedo, and the fraction of land covered by vegetation when the surface is snow-free.

[8] Gusts are defined by WMO as wind extremes that are observed after smoothing the fast signal from an anemometer by a three second running average. The reporting practise is such that gusts are reported as extremes over the previous one, three or six hours. The mean wind is reported as a ten minute average, which is the last ten-minute interval of the hour. The latter should be comparable with the model ten-meter wind, interpreted as an area average because both the time and spatial averaging operator cancel most of the turbulence spectrum. In the ECMWF model, the wind gusts are parameterized as the sum of the instantaneous 10-m wind speed and a stability dependent turbulent gustiness

$$U_{10gust} = U_{10} + 7.71 U_* f(z_i/L) \tag{1}$$

with

$$f(z/L) = \begin{cases} (1 - 0.021 z_i/L)^{1/3} & \text{for L} < 0 \\ 1 & \text{otherwise} \end{cases} \tag{2}$$

where U_{10} is the mean wind speed at 10 m (close to the lowest model level wind), $U_* = |\tau_0| / \rho^{1/2}$ is the friction velocity (itself a function of the 10-m wind speed, with $|\tau_0|$ the absolute surface stress and ρ the density), z_i is the boundary layer height and L is the Monin-Obukhov length scale. The coefficient 7.71 is for a gust duration of three seconds. The z_i/L (buoyancy driven) part of the expression is negligible at strong winds, so the key input to the gust is U_*. The friction velocity is computed from the lowest model level wind using the profile functions also used in the vertical diffusion scheme

$$U_* = \frac{F_{NLEV}}{\ln[(z_{NLEV} + z_0)/z_0] - \Psi_m[(z_{NLEV} + z_0)/L] + \Psi_m(z_0/L)} \tag{3}$$

where F_{NLEV} is the wind speed and z_{NLEV} the height of the lowest model level, Ψ_m is the wind profile stability function and z_0 is the surface roughness length. Again, for strong winds, the Ψ_m functions can be neglected. Overall the gusts are proportional to the mean wind at the lowest model level, with the proportionality factor depending on the roughness length. This factor is small for smooth surfaces (weak turbulence) and large for rough surfaces. The gusts are computed every time-step and estimate the maximum wind (3 s average) within a one hour period (which is of the order of the model time-step).

3. Results

[9] For the month of May 2003, Figure 1 presents, over ocean and land respectively, the global distribution of the monthly mean wind at 10 meters (10W) and the corresponding distribution of the wind at 10 meters including the gustiness (10*WIG*) as discussed above. Figure 1 shows that the gustiness over ocean can add 20 to 25 percent to the amplitude of the wind in areas of strong surface wind (the Southern hemisphere storm track) but more than 50 percent in low wind areas such as off-coast of Liberia, Sierra Leone (6°N, 16°W) and of South Mexico (16°N, 100°W). Similarly, over land, considering gustiness increases the amplitude of the surface wind by more than 50 percent over areas of low wind (Amazonia, Central Africa) and by 25 to 30 percent over North Sahara, South

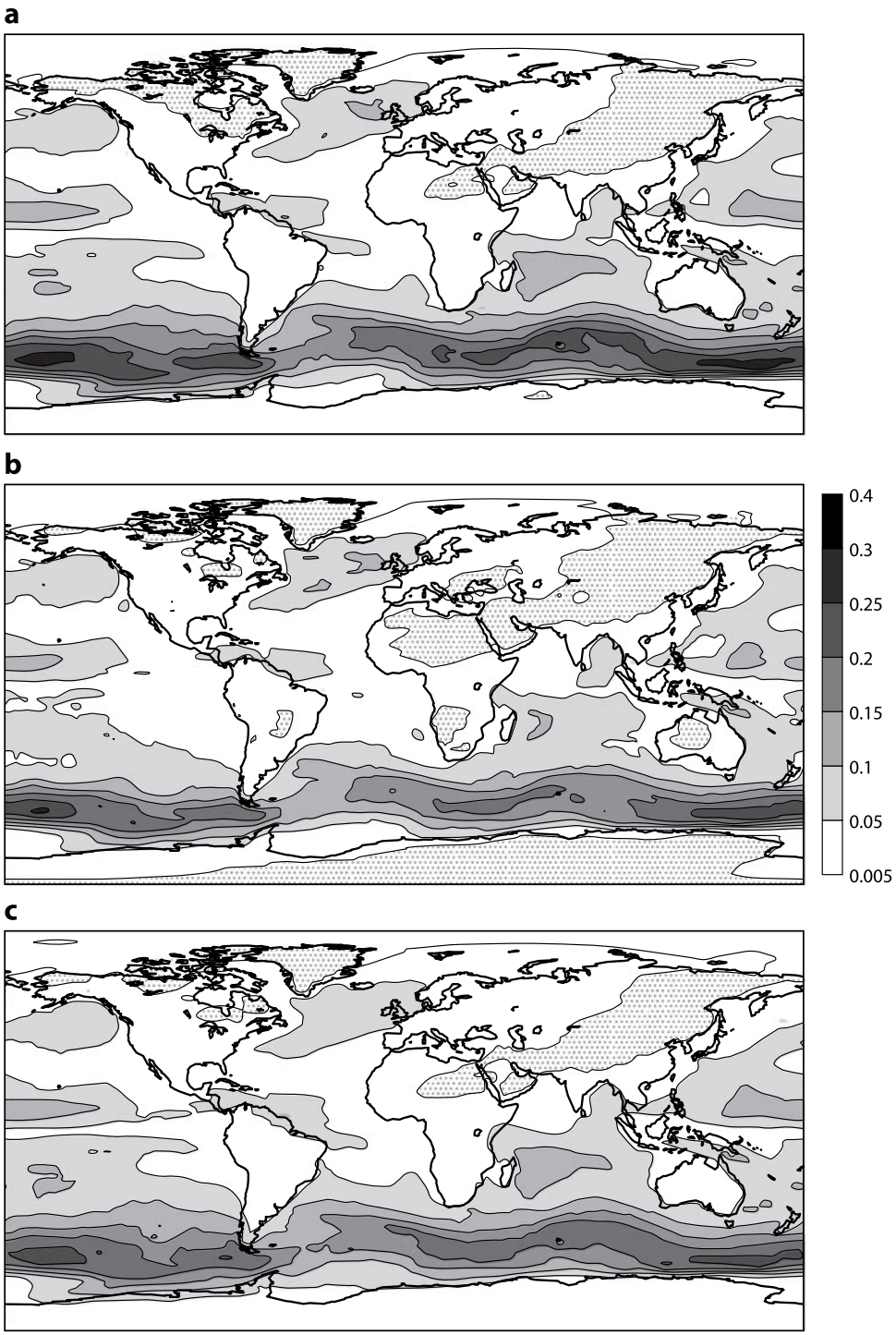

Figure 2. The optical depth at 550 nm of the sea salt component. (a) The free-running forecast. (b) The analysis. (c) The free-running model revised and calibrated on the analysis results.

Central USA, South Argentina and all over South West Asia from Pakistan and India to West China. If a source function following *Monahan et al.* [1982] is used for diagnosing the emission of sea salt, the power 3.41 applied to the surface wind would roughly double the emission when using 10*WIG* instead of 10*W*. Therefore, from comparison of the pdf's of 10*W* and 10*WIG* and that of the *FRA* and *AN* SS, a globally defined normalization factor around 0.5 has been introduced in the parameterization of the emission of sea salt aerosols when using 10*WIG* as predictor. For dust production, the IFS makes the production of dust aerosols proportional to the dust emission potential (*DEP*, which is a function of the soil type and soil moisture) and to $(V - LTS)V^2$ where V is either 10*W* or 10*WIG*, *LTS* is the lifting threshold speed depending on the mean radius of the particle, soil moisture, the UV-visible component of the

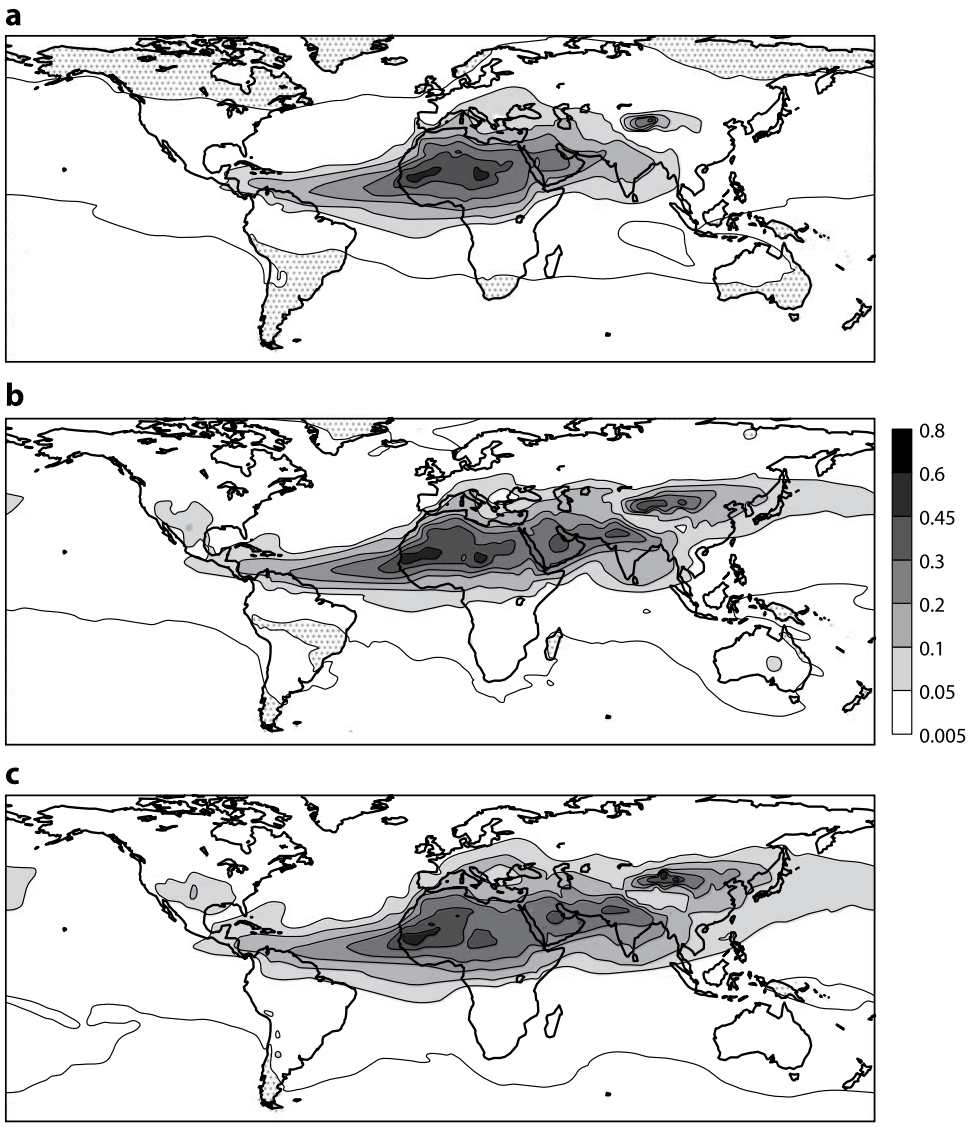

Figure 3. The optical depth at 550 nm of the dust component. (a) The free-running forecast. (b) The analysis. (c) The free-running model revised and calibrated on the analysis results.

surface albedo from MODIS, and the fraction of cover by vegetation when the surface is snow-free. When using 10WIG as predictor, a normalization factor similar to the one for sea salt emission is also used. Figures 2 and 3 present, averaged over May 2003, for the sea salt and dust component respectively, the optical depth at 550 nm (τ_{550}) from the free-running forecast model, the corresponding quantity from the analysis of MODIS optical depth, and the free-running forecast model with the revised formulation calibrated on the analysis results. The revised formulations clearly allow the free-running model to get in much better agreement with the analysis, both for sea salt and dust aerosols. The improvement in τ_{550}^{SS} for sea salt is obtained simply using 10*WIG* as discussed above. The improvement is seen over the areas of strong wind (South Hemisphere storm track) but also in the subtropical areas. For dust, the revised formulation not only uses 10*WIG* but also the geographically relevant DEP's adjusted to give the best agreement possible with the analyzed τ_{550}^{DU} for dust, with the adjustment empirically based on improving on a regional basis the day-to-day *FRA* model τ_{550} w.r.t. to both the MODIS-observed and the AN τ_{550}'s. The revised model clearly improves the distribution of τ_{550}^{DU} from Saudi Arabia to India, and over Northern China. It also makes dust appearing over the South West USA, around the Atacama desert and Australia. Figure 4 compares over the month of May 2003 the time-series of τ_{550}^{SS} and τ_{550}^{DU} from *FR*0, *AN* and *FRA*, with the τ_{500} measured for some AERONET (AErosol RObotic NETwork) stations [*Holben et al.*, 1998] where either sea salt or dust aerosols are prevailing. Those stations were selected based on both the observed Angstrom exponent and the model τ_{550}^{SS} or τ_{550}^{DU} being at least 90 percent of the model total τ_{550}. For example, over Amsterdam Island, FRA provides a smaller τ_{550}^{SS} than FR0. Over Nauru, FRA provides a slightly larger τ_{550}^{SS} than FR0. In all cases, FRA optical depth is closer to AN optical depth. Similar results are also found for dust, with FRA in

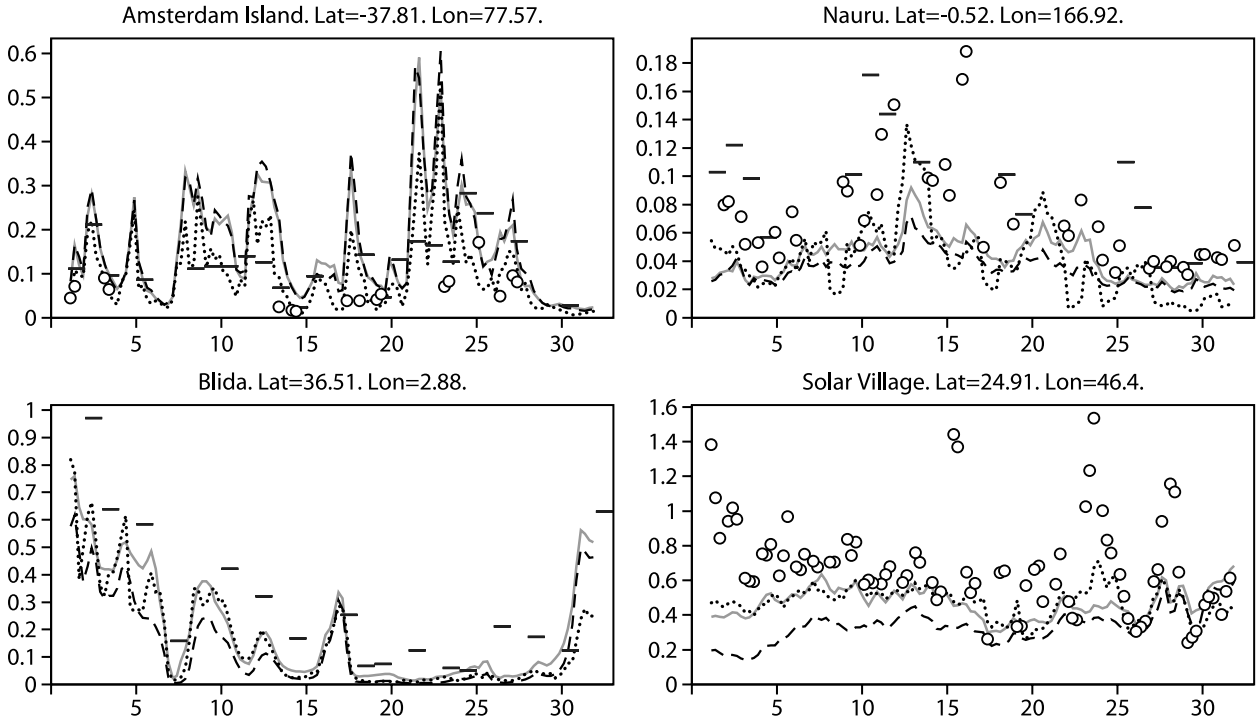

Figure 4. (top left) Time-series of the aerosol optical depth over the AERONET stations, of Amsterdam Island (37.81S–77.57E), (top right) Nauru (0.52S–166.92E), (bottom left) Blida (36.51N–2.88E) and (bottom right) Solar Village (24.91N–46.40E). AERONET observations of aerosol optical depth at 500 nm are given by open circles, the MODIS-derived optical depth at 550 nm by horizontal segments, and the model results are given by dashed, full and dotted lines for FR0, AN and FRA, respectively.

closer agreement with AN than FR0, with a general increase of τ_{550}^{DU}.

4. Conclusion

[10] In this study, the ECMWF IFS was integrated including a prognostic representation of aerosols. Comparisons were made of τ_{550} for sea salt and dust from 12-hour forecasts with free-running aerosols, from an analysis of meteorological observations including MODIS aerosol optical depth, and from forecasts with an improved representation of the sea salt and dust aerosols using the 10 meter wind including gustiness and revised source parameterizations calibrated on the analysis results. This approach to improving the representation of aerosols is clearly successful and could lead to an improved knowledge of the four-dimensional distribution of various aerosols. This study has concentrated on natural aerosols, whose sources are interactive with the rest of the model. A related approach could be used to improve the representation of other aerosols: For example, aerosol plumes of a dominant type could be identified from the analysis of aerosol-sensitive satellite data, similarly tracked and such tracking could help in identifying their sources.

[11] **Acknowledgments.** Observational data for the individual stations in Figure 4 were obtained from the AERONET web site. Brent Holben and his collaborators are thanked for their efforts in establishing and maintaining the AERONET sites used in this study. The MODIS data used as part of the analysis were downloaded from the NASA Giovanni server.

References

Benedetti, A., et al. (2008), Aerosol analysis and forecast in the ECMWF Integrated Forecast System: Data assimilation, *ECMWF Tech. Memo.* 571, pp. 1–25, Eur. Cent. for Medium Range Weather Forecasts, Reading, U. K. (Available at http://www.ecmwf.int/publications/library/do/references/list/14).

Engelstaedter, S., and R. Washington (2007), Temporal controls on global dust emissions: The role of surface gustiness, *Geophys. Res. Lett.*, *34*, L15805, doi:10.1029/2007GL029971.

Ginoux, P., M. Chin, I. Tegen, J. Prospero, B. N. Holben, O. Dubovik, and S.-J. Lin (2001), Sources and distributions of dust aerosols simulated with the GOCART model, *J. Geophys. Res.*, *106D*, 20,255–20,273.

Holben, B. N., et al. (1998), An emerging ground-based aerosol climatology: Aerosol optical depth from AERONET, *J. Geophys. Res.*, *106*, 12,067–12,097.

Marenco, F., F. Mazzei, P. Prati, and M. Gatti (2007), Aerosol advection and sea salt events in Genoa, Italy, during the second half of 2005, *Sci. Total Environ.*, *377*, 396–406.

Monahan, E. C., K. L. Davidson, and D. E. Spiel (1982), Whitecap aerosol productivity deduced from simulation tank measurements, *J. Geophys. Res.*, *87*, 8898–8904.

Morcrette, J.-J., et al. (2008), Aerosol analysis and forecast in the ECMWF Integrated Forecast System: Data assimilation, *ECMWF Tech. Memo.* 573, pp. 1–35, Eur. Cent. for Medium Range Weather Forecasts, Reading, U. K. (Available at http://www.ecmwf.int/publications/library/do/references/list/14).

A. Benedetti, A. Beljaars, L. Jones, and J.-J. Morcrette, ECMWF, Shinfield Park, Reading, RG2 9AX, UK. (pam@ecmwf.int)

O. Boucher, Met Office, Hadley Centre, FitzRoy Road, Exeter, EX1 3PB, UK.